SUPPLEMENTARY MATERIAL

Targeted suppression of miRNA-33 using pHLIP improves atherosclerosis regression

Xinbo Zhang, Noemi Rotllan, Alberto Canfrán-Duque, Jonathan Sun, Jakub Toczek, Anna Moshnikova, Shipra Malik, Nathan L. Price. Elisa Araldi, Wen Zhong, Mehran M. Sadeghi, Oleg A. Andreev, Raman Bahal, Yana Reshetnyak, Yajaira Suárez, Carlos Fernández-Hernando.

SUPPLEMENTAL FIGURE LEGENDS

Figure S1. pH low inducible peptides (pHLIP) are highly internalized in atherosclerotic plaques. A-B, Representative images (**A**) and quantification (**B**) of tissues from low density lipoprotein receptor knockout (*Ldlr*$^{-/-}$) mice injected with fluorescently labeled targeted (A546-Var3) or non-inserting control (A546-5K-Var3) constructs. *Ldlr*$^{-/-}$ mice were fed a western diet (WD) for 3 months to induce atherosclerosis and tissues were harvested 4-24 hours post injection of constructs. **C**, Representative images demonstrating uptake of A546-Var3 into liver and kidney with A546-5K-Var3 as control. Scale bar: 100 μm.

Figure S2. pH low insertion peptides (pHLIP) do not target CD45^{-} cells in atherosclerotic plaques. A, Representative flow cytometry histograms showing fluorescence intensities in CD45^{-} cells isolated from atherosclerotic lesions of mice injected with PBS, A546-5K-Var3 or A546-Var3 constructs. **B**, Quantification of the median fluorescence intensity [MFI; arbitrary units (a.u.)] and % of A546^{+} CD45^{-} cells is shown in right panels. Quantification represents the mean ± SEM (n=4 in A546-5K-Var3 and n=5 in A546-Var3 group). Data normality was assessed using Shapiro-Wilk test and analyzed by an unpaired two-sided Student's t-test.

Figure S3. pH low inducible peptides (pHLIP) are not internalized by spleen and lung monocytes from hypercholesterolemic mice. *Ldlr*$^{-/-}$ mice were fed a western diet (WD) for 3 months to induce atherosclerosis and tissues were harvested 4 hours post injection of constructs. **A,** Representative images of tissues from low density lipoprotein receptor knockout (*Ldlr*$^{-/-}$) mice injected with fluorescently labeled targeted (A750-Var3) or non-inserting control (A750-5K-Var3) constructs. **B**, Representative flow cytometry histograms of fluorescence intensities in spleen and lung monocytes from mice injected with A546-5K-Var3 (control) or A546-Var3 constructs.

Figure S4. Selective targeting of miR-33-5p using pHLIP does not affect cellular viability and lipid uptake but increases cholesterol efflux in macrophages. A-B, anti-miR-33-5p peptide nucleic acid delivery vector (anti-miR33^{pHLIP}) does not influence cellular viability measured by MTT analysis (**A**) and DiI-labeled acetylated low-density lipoprotein (DiI-Ac-LDL, 10 mg/ml) uptake under neutral (pH 7.4) and acidic (pH 6.2) conditions (**B**). **C**, anti-miR33^{pHLIP} uptake increased cholesterol efflux to apolipoprotein A1 (ApoA1) in macrophages cultured in neutral (pH 7.4) and acidic (pH 6.2) conditions. **D**, pHLIP uptake in foamy and non-foamy macrophages isolated from low-density lipoprotein receptor knockout (*Ldlr*$^{-/-}$) mice fed a chow diet (CD) and western diet (WD) and injected with fluorescently labeled targeted (A633-Var3) peptide. **E**, % of pHLIP (A633-Var3) positive macrophages from *Ldlr*$^{-/-}$ mice fed with a WD compared to animals fed with a CD. Quantification represents the mean ± SEM (n= 3 per group). Data were analyzed by one-way ANOVA (**A** and **B**), two-way ANOVA (**C**) with Bonferroni correction for multiple comparisons or a nonparametric Mann-Whitney test after data normality analysis using Shapiro-Wilk test (**D** and **E**).

Figure S5. miR-33 silencing using anti-miR33^{pHLIP} **enhances ABCA1 expression and attenuates neutral lipid accumulation in human macrophages derived from THP-1 cells**. **A**, Flow cytometry analysis showing the uptake of A633-5K-Var3 (con) or A633-Var3 constructs in

THP-1 cells. MFI: median fluorescence intensity. **B**, Representative Oil-red O (ORO) staining of THP-1 macrophages treated with anti-miR-33^{pHLIP} or Scr^{pHLIP} and incubated with acetylated low-density lipoprotein (Ac-LDL). Quantification of lipid accumulation is shown in the right panel. **C**, Representative Western blot analysis of ABCA1 in THP-1-derived macrophages incubated with anti-miR-33^{pHLIP} or Scr^{pHLIP} for 24 and 48 hours. Quantification shown in the right panel. Quantification represents the mean ± SEM (n= 3 per group). Data were analyzed by a nonparametric Mann-Whitney test (**A** and **B**) or two-way ANOVA (**C**) with Bonferroni correction for multiple comparisons or after data normality analysis using Shapiro-Wilk test.

Figure S6. Targeted silencing of miR-33-5p does not influence circulating lipids, lipoprotein profiles and body weight. A, Plasma total cholesterol, high density lipoprotein (HDL) cholesterol and triglycerides from low-density lipoprotein receptor knockout (*Ldlr*$^{-/-}$) mice injected with anti-miR33^{pHLIP}) or Scr^{pHLIP} (n=17 in Baseline, n=13 in Scr^{pHLIP} and anti-miR-33^{pHLIP} group). **B**, FPLC analysis of circulating lipoproteins from *Ldlr*$^{-/-}$ mice injected anti-miR33^{pHLIP} or Scr^{pHLIP}. **C**, Body weight of *Ldlr*$^{-/-}$ mice injected anti-miR33^{pHLIP} or Scr^{pHLIP} (n=17 in Baseline, n=13 in Scr^{pHLIP} and n=14 in anti-miR-33^{pHLIP} group). Quantification represents the mean ± SEM. Data were analyzed by one-way ANOVA with Bonferroni correction for multiple comparisons.

Figure S7. Selective targeting of miR-33-5p using pHLIP peptides does not affect circulating leukocytes and hepatic function. A, Quantification of peripheral blood counts by hemocytometer from *Ldlr*$^{-/-}$ mice injected with anti-miR33^{pHLIP} or scrambled control Scr^{pHLIP} (n=8 per group). **B**, Quantification of serum hepatotoxicity markers, aspartate aminotransferase (AST) and alanine aminotransferase (ALT), from *Ldlr*$^{-/-}$ mice injected anti-miR33^{pHLIP} or Scr^{pHLIP} (*n*=7 per group). Quantification represents the mean ± SEM. Data were analyzed by two-way ANOVA with

Bonferroni correction for multiple comparisons (**A**) and an unpaired two-sided Student's t-test after data normality analysis using Shapiro-Wilk test (**B**).

Figure S8. Antagonist miR-33 expression using anti-miR33^{pHLIP} **does not influence hepatic ABCA1 and ABCG1 expression. A,** miR-33 expression in liver, spleen, lung and kidney isolated from *Ldlr*$^{-/-}$ mice injected intravenously with anti-miR33^{pHLIP} or Scr^{pHLIP} at a dose of 1 mg/kg body weight (*n*= 4 in Scr^{pHLIP} and n=6 in anti-miR33^{pHLIP} group). **B**, Representative Western blot analysis of ABCA1 and ABCG1 in the liver, spleen, lung, and kidney from *Ldlr*$^{-/-}$ mice injected with anti-miR-33-5p^{pHLIP} or Scr^{pHLIP}. Quantification is shown in the bottom panels (n=5). Data normality was assessed using Shapiro-Wilk test and analyzed by an unpaired two-sided Student's t-test. Quantification represents the mean ± SEM.

Figure S9. scRNA-Seq analysis of aortic cells from *Ldlr*$^{-/-}$ mice treated with treated anti-miR33^{pHLIP} or Scr^{pHLIP}. A, Heatmap of the 20 most upregulated genes in each cluster defined in **Figure 5A** and selected enriched genes used for biological identification of each cluster. **B**, Distribution of cells extracted from the atherosclerotic aortas of anti-miR33^{pHLIP} and Scr^{pHLIP}-treated mice.

Figure S10. Gene expression features from indicated monocytes/macrophages clusters. A, Uniform manifold approximation and projection (UMAP) plots of *Cd14, Cd68, Adgre1*, and *Csf1r* in sorted cells from atherosclerotic plaques of mice treated with anti-miR33^{pHLIP} or Scr^{pHLIP}. **B**, UMAP plots of most highly upregulated genes for clusters of Trem2^{high} Mac, F10^{+} Mono, Inflammatory Mac and Stem-like Mac. **C**, UMAP plots of most highly upregulated genes for ECM^{high} Mac cluster. Dot intensity values is represented in arbitrary unit in the Y axis.

Table S1. Key resources used in this study.

REAGENT or RESOURCE	SOURCE	IDENTIFIER
Antibodies		
anti-ABCA1	Abcam	ab18180
anti-ABCG1	Novus Biologicals	NB400-132
anti-CD11b	BioLegend	#101212
anti-CD31	BioLegend	#102422
anti-CD45	BioLegend	#103112
anti-CD68	Serotec	#MCA1957
anti-CD115	BioLegend	#135506
anti-F4/80	BioLegend	#123108
anti-HSP90	BD Biosciences	#610419
anti-Ly6-C	BD Biosciences	#128018
anti-Ly6-G	BioLegend	#127613
anti-αSMA	Sigma-Aldrich	#C6198
Rat IgG2a negative control	Bio-Rad	MCA1212
FITC-conjugated Goat anti-Rat IgG	ThermoFisher	#31629
Chemicals, Peptides, and Recombinant Proteins		
acLDL	ThermoFisher	L35354
Recombinant human apolipoprotein AI	Abcam	Ab50239
[1,2-3H(N)]-Cholesterol	PerkinElmer	NET139250UC
Collagenase A	Roche	#11088785103
DiI-acLDL	ThermoFisher	L3484
Elastase	Worthington	LS006365
eBioscience™ Fixable Viability Dye eFluor™ 450	ThermoFisher	#65-0863-14
Oil-Red O	Sigma-Aldrich	O0625
PMA	Sigma-Aldrich	P1585
RPMI 1640 medium	ThermoFisher	#21875034
Critical Commercial Assays		
ALT Activity Assay	Sigma-Aldrich	MAK052-1KT
AST Activity Assay Kit	Sigma-Aldrich	MAK055-1KT
Cholesterol E	Wako	#999-02601

L-Type Triglyceride M	Wako	#996-02895; #992-02995
HDL Cholesterol E	Wako	#431-52501
DC™ protein assay kit	BioRad	#5000111
CyQUANT™ MTT Cell Viability Assay	Invitrogen	V13154
miR33 primers	Qiagen	#339306, GeneGlobe YP00205690
U6 primers	Qiagen	#339306, GeneGlobe YP02119464
RNeasy Mini Kit	Qiagen	#74104
RNeasy MinElute Cleanup Kit	Qiagen	#74204
Chromium Single Cell 3′ v2	10X Genomics	#120237
Deposited Data		
Single cell RNA sequencing data	This paper	GEO (#GSE191220)
Experimental Models: Cell Lines		
THP-1	ATCC	TIB-202
Experimental Models: Organisms/Strains		
Wild type mice	The Jackson Laboratory	000664
Ldlr knockout mice	The Jackson Laboratory	002207
Software and Algorithms		
FlowJo v10	FlowJo, LLC	https://www.flowjo.com/
Prism 7.0	GraphPad Software	https://www.graphpad.com/
Image J v1.51	NIH	https://imagej.nih.gov/ij/
CellRanger v2.1.1	10x Genomics	https://www.10xgenomics.com
R v3.6.1	R Core team	www.R-project.org
Seurat v3.2.0	(Stuart et al., 2019)	https://www.satijalab.org/seurat
Ingenuity® Pathways Analysis™ (IPA) v47547484	Qiagen	https://www.qiagen.com/
Other		
western diet (40% fat and 1.25% cholesterol)	ResearchDiets	D12108

Table S2. Primer sequences for qPCR analysis.

mRNA	Primer sequences
Abca1	5'-GGTTTGGAGATGGTTATACAATAGTTGT-3' 5'-CCCGGAAACGCAAGTCC-3'
Gapdh	5'- AGGTCGGTGTGAACGGATTTG-3' 5'- TGTAGACCATGTAGTTGAGGTCA-3'

Table S3. Differentially expressed genes (DEs) in Mono/Mac clusters.

	p_val	avg_logFC	Anti-miR33	Src	p_val_adj
H2-Eb1	1.85E-20	0.5095993	0.538	0.389	2.78E-16
H2-Aa	5.60E-19	0.4614027	0.533	0.392	8.44E-15
Ly6e	5.63E-19	0.4058898	0.517	0.391	8.48E-15
H2-Ab1	4.21E-16	0.4465454	0.573	0.461	6.34E-12
H2-K1	8.52E-16	0.3204827	0.874	0.853	1.28E-11
Col1a2	9.92E-15	0.6335151	0.523	0.431	1.50E-10
Cd74	2.89E-14	0.4368148	0.764	0.702	4.35E-10
Ifitm3	6.65E-14	0.3149755	0.561	0.45	1.00E-09
Timp3	8.77E-13	0.3719783	0.333	0.232	1.32E-08
Comp	7.69E-12	0.5019428	0.445	0.345	1.16E-07
Sparc	9.89E-12	0.59755	0.973	0.973	1.49E-07
Mmp12	4.36E-11	-0.4083571	0.348	0.45	6.57E-07
Col1a1	5.49E-11	0.3609094	0.44	0.351	8.28E-07
Col3a1	2.30E-10	0.2562241	0.46	0.382	3.47E-06
Bgn	6.61E-10	0.4516121	0.64	0.594	9.96E-06
Nupr1	4.07E-09	0.2916874	0.6	0.552	6.13E-05
Col2a1	1.49E-07	0.8909633	0.425	0.364	2.25E-03
Fn1	1.61E-06	0.3528053	0.675	0.631	2.43E-02
Bst2	1.64E-06	0.297678	0.578	0.555	2.47E-02

Table S4. Ingenuity pathway analysis from upregulated differentially genes in Mono/Mac clusters.

Ingenuity Canonical Pathways	-log(p-value)	p value	Ratio
Dendritic Cell Maturation	11.7	1.84E-12	0.0435
Antigen Presentation Pathway	9.76	1.73E-10	0.128
Apelin Liver Signaling Pathway	8.19	6.44E-09	0.154
B Cell Development	7.6	2.52E-08	0.111
Intrinsic Prothrombin Activation Pathway	7.32	4.78E-08	0.0952
Graft-versus-Host Disease Signaling	7.08	8.27E-08	0.0833
Autoimmune Thyroid Disease Signaling	7.05	9E-08	0.0816
Calcium-induced T Lymphocyte Apoptosis	6.52	3.03E-07	0.0606
T Helper Cell Differentiation	6.34	4.56E-07	0.0548
Hepatic Fibrosis / Hepatic Stellate Cell Activation	6.31	4.88E-07	0.0269
Natural Killer Cell Signaling	6.19	6.49E-07	0.0254
IL-4 Signaling	6.07	8.43E-07	0.0471
Allograft Rejection Signaling	6.05	8.84E-07	0.0465
Altered T Cell and B Cell Signaling in Rheumatoid Arthritis	5.97	1.06E-06	0.0444
OX40 Signaling Pathway	5.97	1.06E-06	0.0444
PD-1, PD-L1 cancer immunotherapy pathway	5.69	2.04E-06	0.0377
iCOS-iCOSL Signaling in T Helper Cells	5.61	2.46E-06	0.036
Type I Diabetes Mellitus Signaling	5.61	2.46E-06	0.036
GP6 Signaling Pathway	5.49	3.24E-06	0.0336
CD28 Signaling in T Helper Cells	5.46	3.47E-06	0.0331
Th1 Pathway	5.46	3.47E-06	0.0331
Atherosclerosis Signaling	5.38	4.2E-06	0.0315
Th2 Pathway	5.26	5.52E-06	0.0294
PKCθ Signaling in T Lymphocytes	5.03	9.26E-06	0.0258
Th1 and Th2 Activation Pathway	4.87	1.36E-05	0.0234
T Cell Exhaustion Signaling Pathway	4.83	1.49E-05	0.0229
Cdc42 Signaling	4.82	1.53E-05	0.0227
Tumor Microenvironment Pathway	4.82	1.53E-05	0.0227
Role of NFAT in Regulation of the Immune Response	4.77	1.71E-05	0.0221
Osteoarthritis Pathway	4.44	3.66E-05	0.0182
Neuroinflammation Signaling Pathway	3.91	1.22E-04	0.0133
MSP-RON Signaling In Macrophages Pathway	3.89	1.28E-04	0.0265
Systemic Lupus Erythematosus In T Cell Signaling Pathway	3.74	1.84E-04	0.012
Hepatic Fibrosis Signaling Pathway	3.54	2.9E-04	0.0106
Crosstalk between Dendritic Cells and Natural Killer Cells	2.56	2.75E-03	0.0225

Communication between Innate and Adaptive Immune Cells	2.5	3.19E-03	0.0208
Phagosome Maturation	2.11	7.7E-03	0.0132
HOTAIR Regulatory Pathway	2.06	8.61E-03	0.0125
Cytotoxic T Lymphocyte-mediated Apoptosis of Target Cells	1.53	2.95E-02	0.0294
MIF-mediated Glucocorticoid Regulation	1.53	2.95E-02	0.0294
Interferon Signaling	1.51	3.12E-02	0.0278
Inhibition of Matrix Metalloproteases	1.47	3.38E-02	0.0256
MIF Regulation of Innate Immunity	1.44	3.63E-02	0.0238
Oncostatin M Signaling	1.43	3.72E-02	0.0233
Coronavirus Replication Pathway	1.41	3.89E-02	0.0222
Caveolar-mediated Endocytosis Signaling	1.21	6.23E-02	0.0137
Glioma Invasiveness Signaling	1.21	6.23E-02	0.0137
CTLA4 Signaling in Cytotoxic T Lymphocytes	1.12	7.55E-02	0.0112
p53 Signaling	1.08	8.28E-02	0.0102
Virus Entry via Endocytic Pathways	1.06	8.61E-02	0.0098
Neuregulin Signaling	1.05	8.85E-02	0.00952
Neuroprotective Role of THOP1 in Alzheimer's Disease	1.01	9.73E-02	0.00862
IL-6 Signaling	0.979	1.05E-01	0.00794
Phagosome Formation	0.955	1.11E-01	0.00752
Endocannabinoid Cancer Inhibition Pathway	0.924	1.19E-01	0.00699
Acute Phase Response Signaling	0.833	1.47E-01	0.00556
ILK Signaling	0.81	1.55E-01	0.00526
Agranulocyte Adhesion and Diapedesis	0.807	1.56E-01	0.00521
Leukocyte Extravasation Signaling	0.804	1.57E-01	0.00518
Role of Osteoblasts, Osteoclasts and Chondrocytes in Rheumatoid Arthritis	0.757	1.75E-01	0.00459
Actin Cytoskeleton Signaling	0.74	1.82E-01	0.00441
Systemic Lupus Erythematosus Signaling	0.738	1.83E-01	0.00437
Protein Ubiquitination Pathway	0.668	2.15E-01	0.00366
Role of Macrophages, Fibroblasts and Endothelial Cells in Rheumatoid Arthritis	0.616	2.42E-01	0.00319
Synaptogenesis Signaling Pathway	0.616	2.42E-01	0.00321

Note: P-value were calculated with Fisher's Exact Test and corrected based on the Benjamini-Hochberg method.

Figure S1

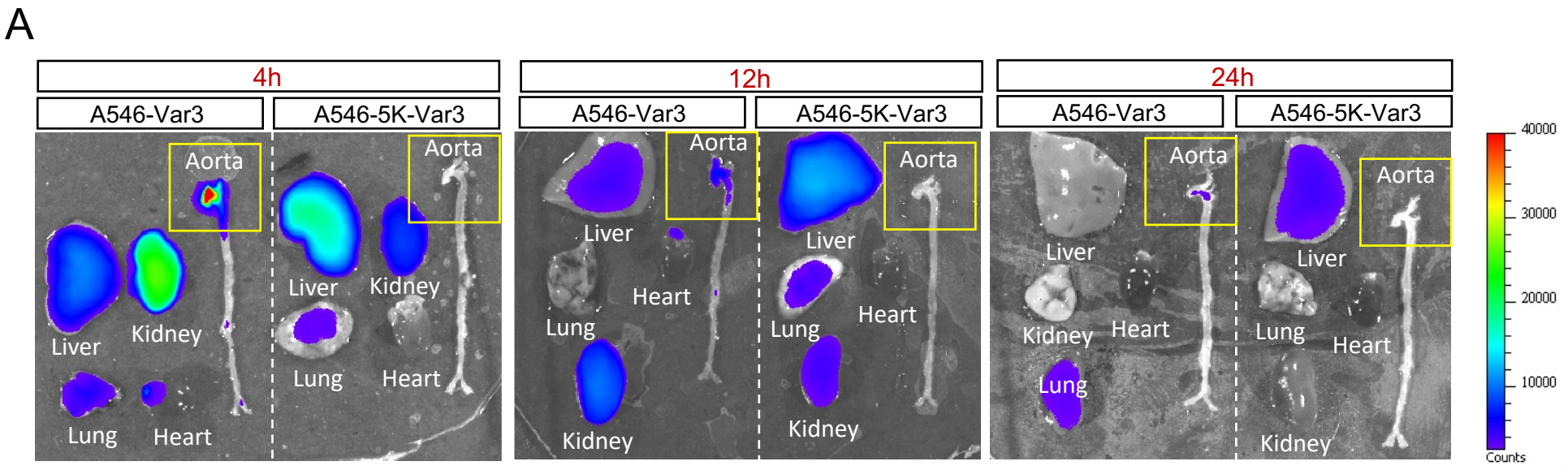
A
4h
12h
24h
A546-Var3
A546-5K-Var3
Aorta
Liver
Kidney
Lung
Heart
40000
30000
20000
10000
Counts

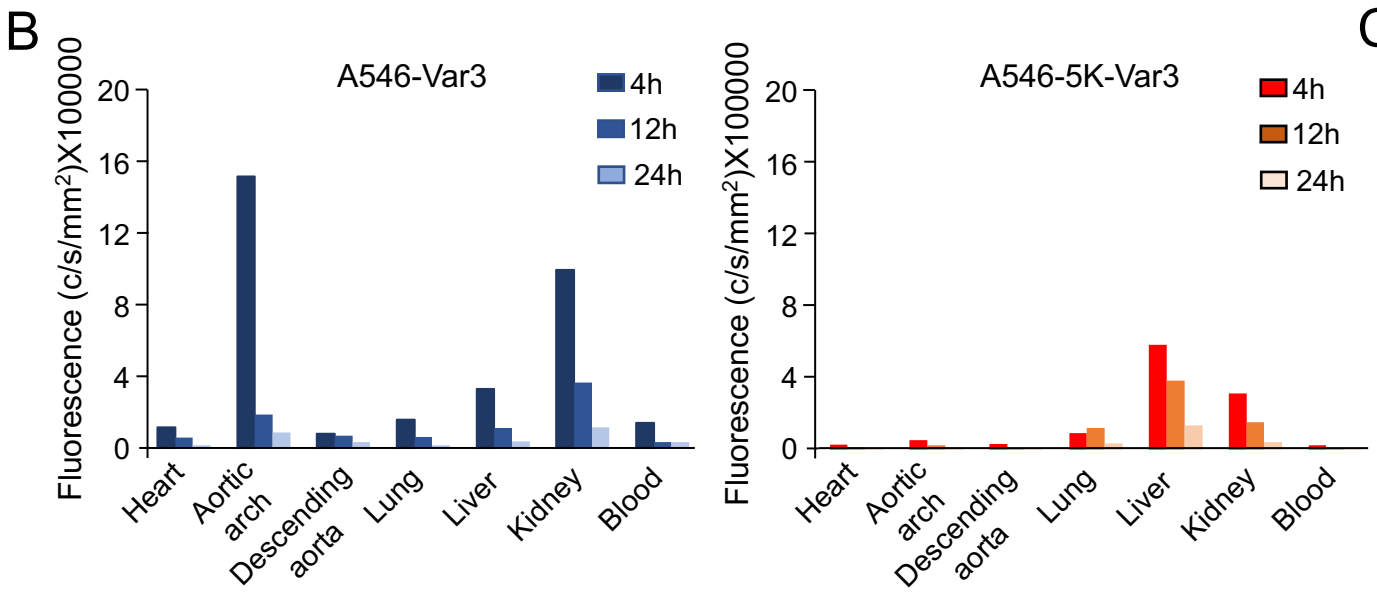
B
A546-Var3
A546-5K-Var3
4h
12h
24h
Fluorescence (c/s/mm²)X100000
20
16
12
8
4
0
Heart
Aortic arch
Descending aorta
Lung
Liver
Kidney
Blood

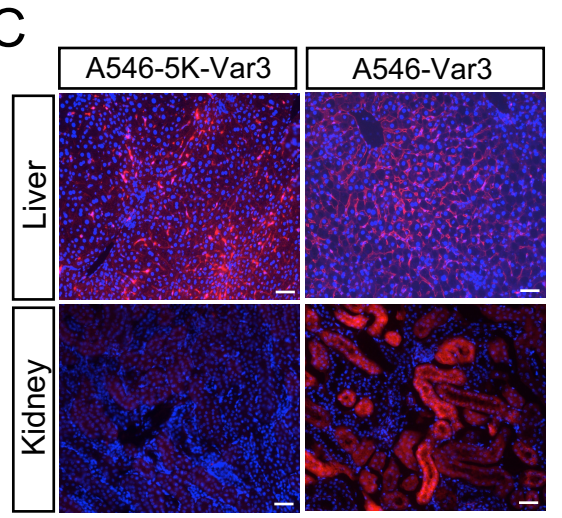
C
A546-5K-Var3
A546-Var3
Liver
Kidney

Figure S2

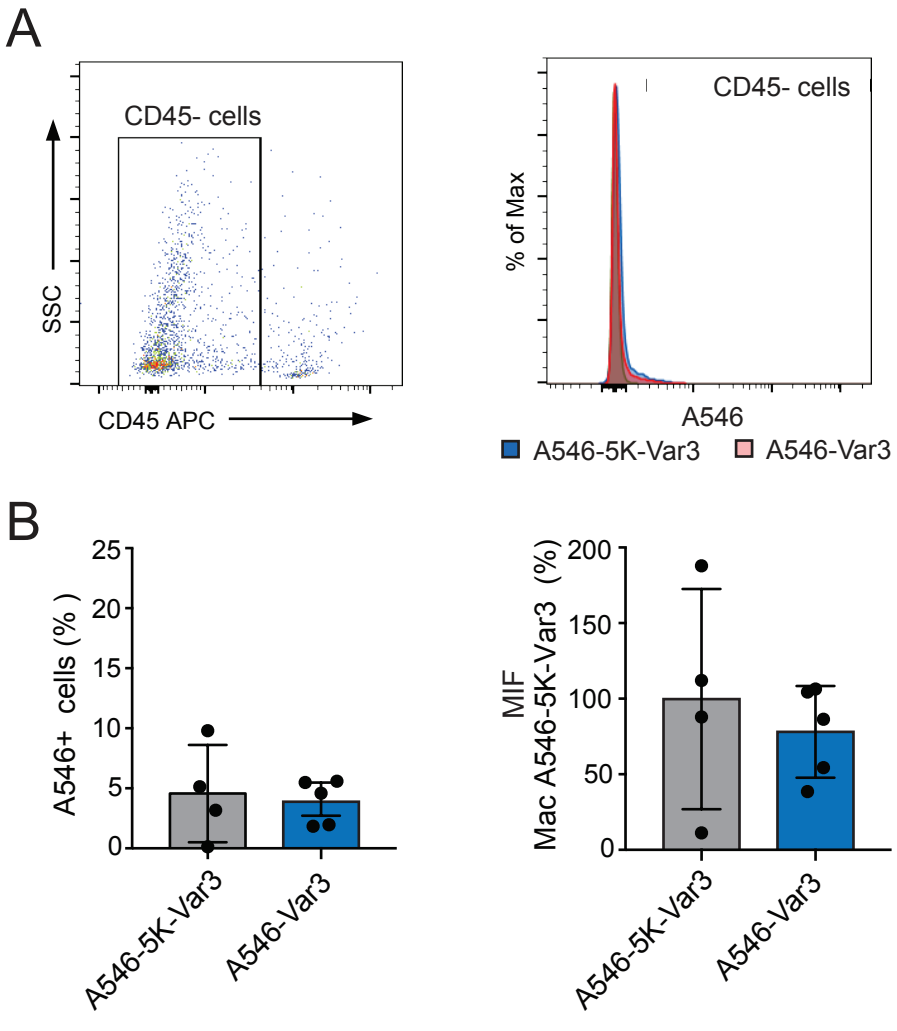
A
CD45- cells
SSC
CD45 APC
CD45- cells
% of Max
A546
A546-5K-Var3
A546-Var3
B
A546+ cells (%)
25
20
15
10
5
0
A546-5K-Var3
A546-Var3
MIF
Mac A546-5K-Var3 (%)
200
150
100
50
0
A546-5K-Var3
A546-Var3

Figure S3

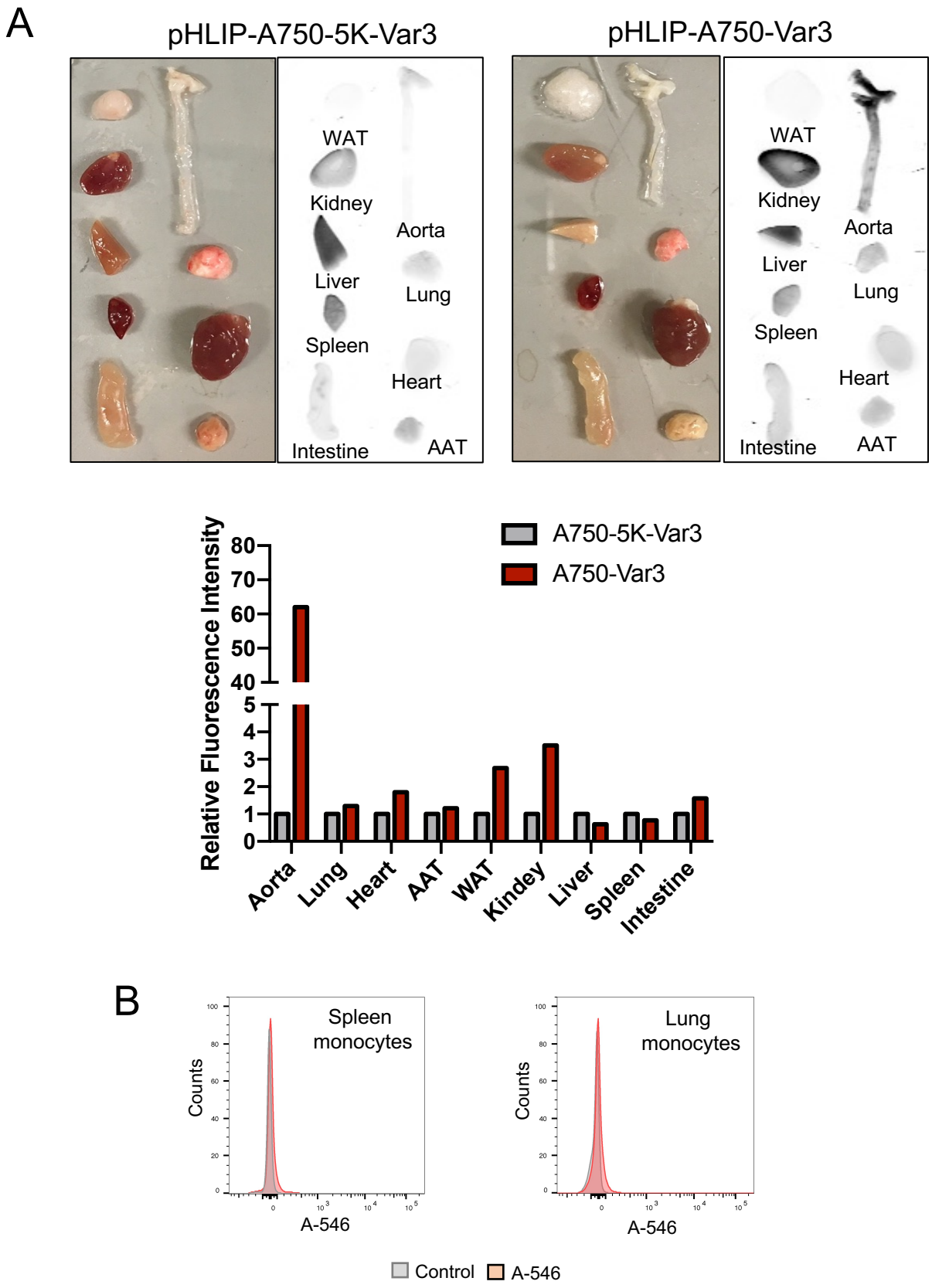
A
pHLIP-A750-5K-Var3
pHLIP-A750-Var3
WAT
Kidney
Liver
Spleen
Intestine
Aorta
Lung
Heart
AAT
A750-5K-Var3
A750-Var3
Relative Fluorescence Intensity
Aorta
Lung
Heart
AAT
WAT
Kindey
Liver
Spleen
Intestine
B
Spleen monocytes
Lung monocytes
Counts
A-546
Control
A-546

Figure S4

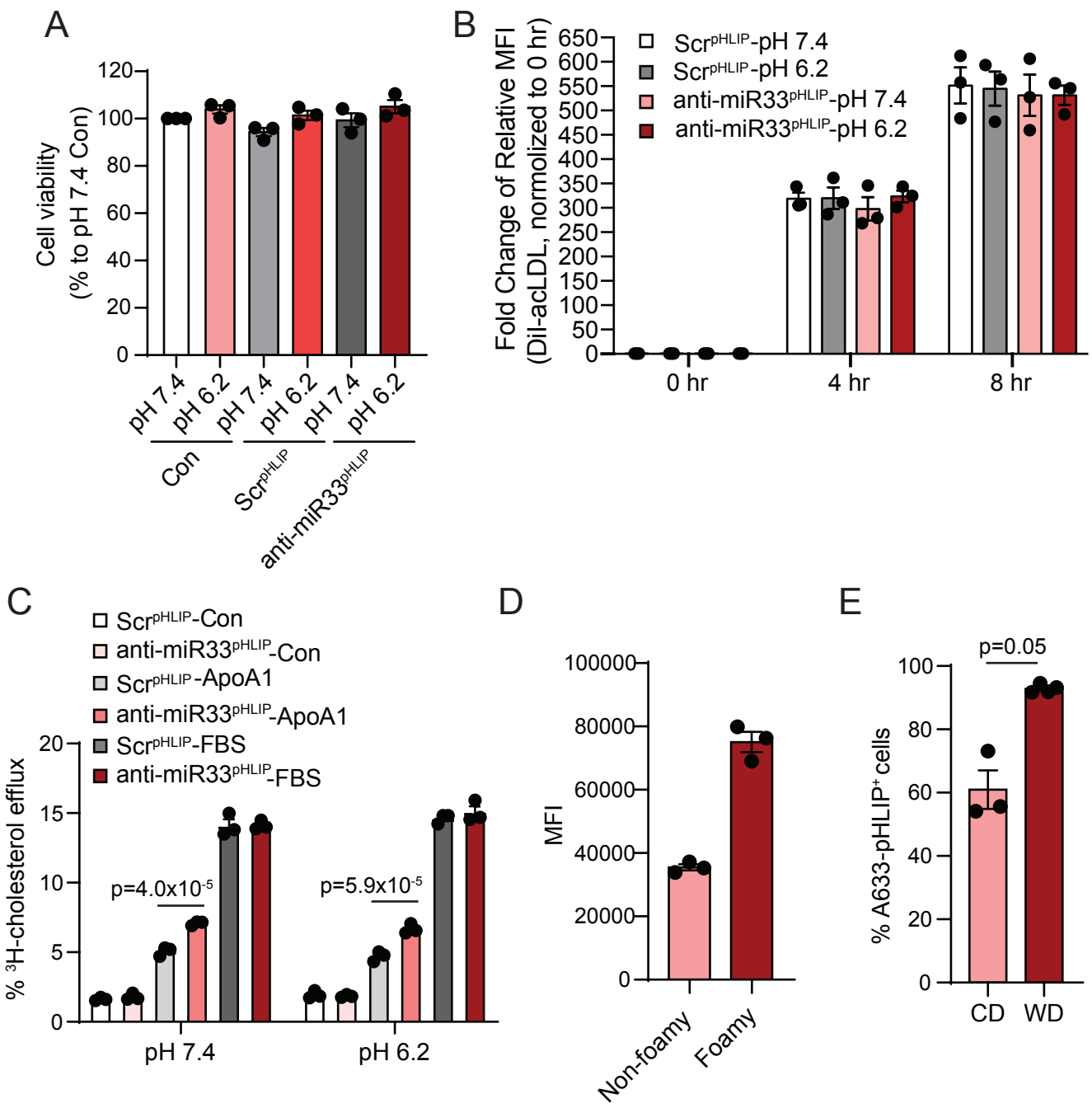
A
Cell viability
(% to pH 7.4 Con)
120
100
80
60
40
20
0
pH 7.4
pH 6.2
pH 7.4
pH 6.2
pH 7.4
pH 6.2
Con
Scr^pHLIP
anti-miR33^pHLIP
B
Fold Change of Relative MFI
(Dil-acLDL, normolized to 0 hr)
650
600
550
500
450
400
350
300
250
200
150
100
50
0
Scr^pHLIP-pH 7.4
Scr^pHLIP-pH 6.2
anti-miR33^pHLIP-pH 7.4
anti-miR33^pHLIP-pH 6.2
0 hr
4 hr
8 hr
C
Scr^pHLIP-Con
anti-miR33^pHLIP-Con
Scr^pHLIP-ApoA1
anti-miR33^pHLIP-ApoA1
Scr^pHLIP-FBS
anti-miR33^pHLIP-FBS
% ³H-cholesterol efflux
20
15
10
5
0
p=4.0x10-5
p=5.9x10-5
pH 7.4
pH 6.2
D
MFI
100000
80000
60000
40000
20000
0
Non-foamy
Foamy
E
% A633-pHLIP+ cells
100
80
60
40
20
0
p=0.05
CD
WD

Figure S5

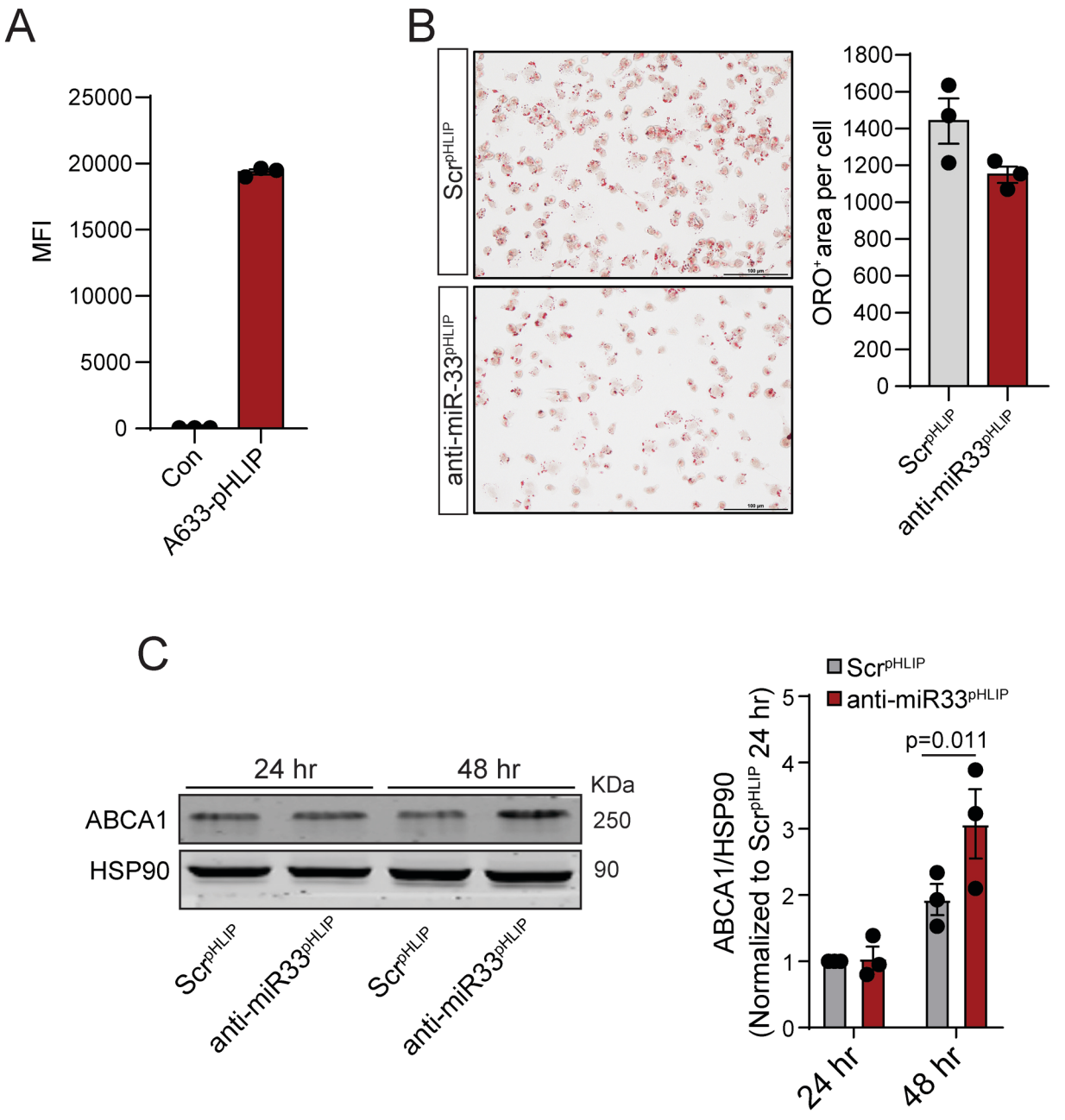
A
MFI
25000
20000
15000
10000
5000
0
Con
A633-pHLIP
B
Scr^pHLIP
anti-miR-33^pHLIP
ORO+ area per cell
1800
1600
1400
1200
1000
800
600
400
200
0
Scr^pHLIP
anti-miR33^pHLIP
C
24 hr
48 hr
KDa
ABCA1
250
HSP90
90
Scr^pHLIP
anti-miR33^pHLIP
Scr^pHLIP
anti-miR33^pHLIP
Scr^pHLIP
anti-miR33^pHLIP
p=0.011
ABCA1/HSP90
(Normalized to Scr^pHLIP 24 hr)
5
4
3
2
1
0
24 hr
48 hr

Figure S6

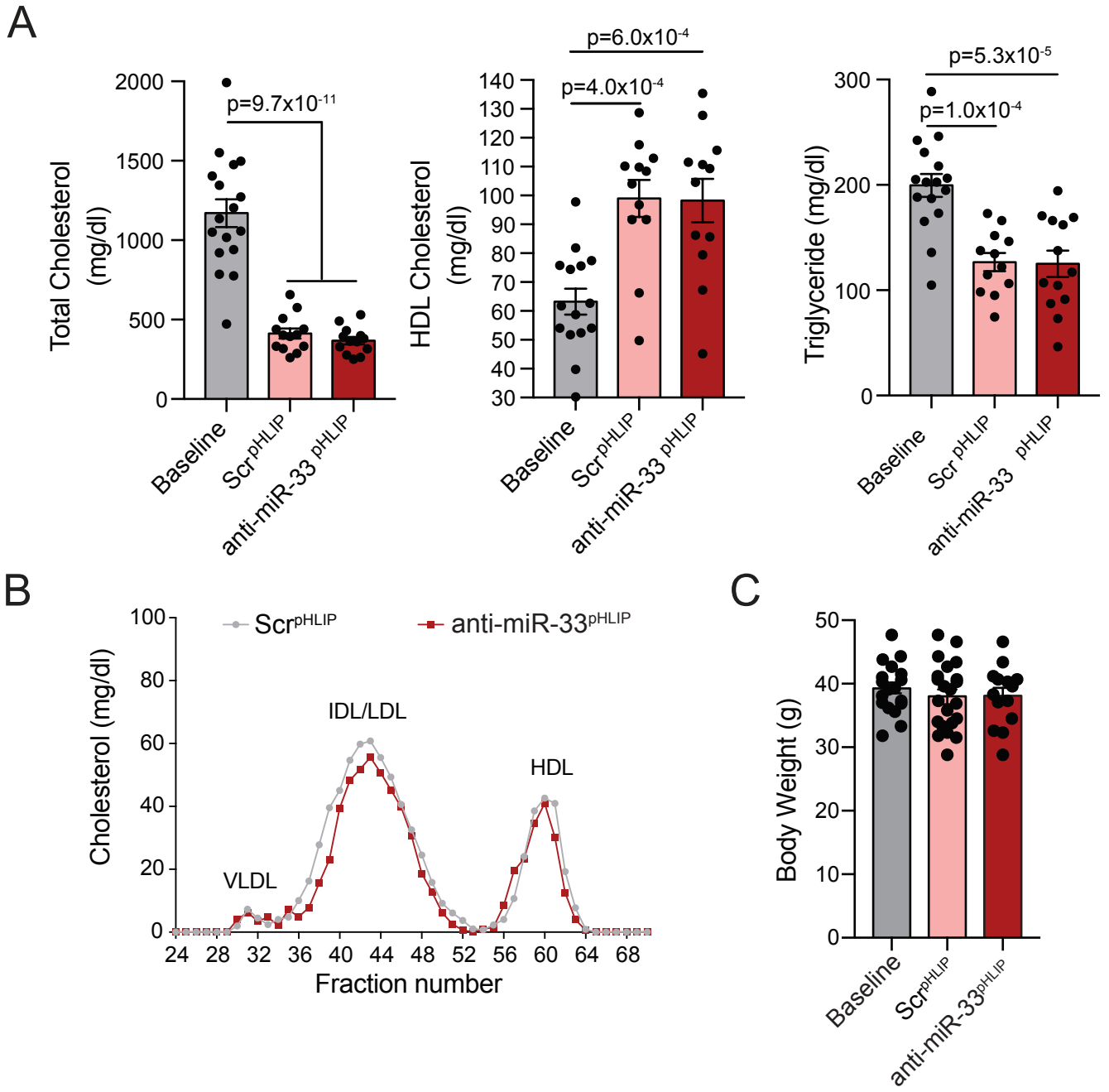
A
Total Cholesterol (mg/dl)
p=9.7x10-11
2000
1500
1000
500
0
Baseline
Scr pHLIP
anti-miR-33 pHLIP
HDL Cholesterol (mg/dl)
p=6.0x10-4
p=4.0x10-4
140
130
120
110
100
90
80
70
60
50
40
30
Triglyceride (mg/dl)
p=5.3x10-5
p=1.0x10-4
300
200
100
0
B
Cholesterol (mg/dl)
Scr pHLIP
anti-miR-33 pHLIP
IDL/LDL
HDL
VLDL
100
80
60
40
20
0
24 28 32 36 40 44 48 52 56 60 64 68
Fraction number
C
Body Weight (g)
50
40
30
20
10
0
Baseline
Scr pHLIP
anti-miR-33 pHLIP

Figure S7

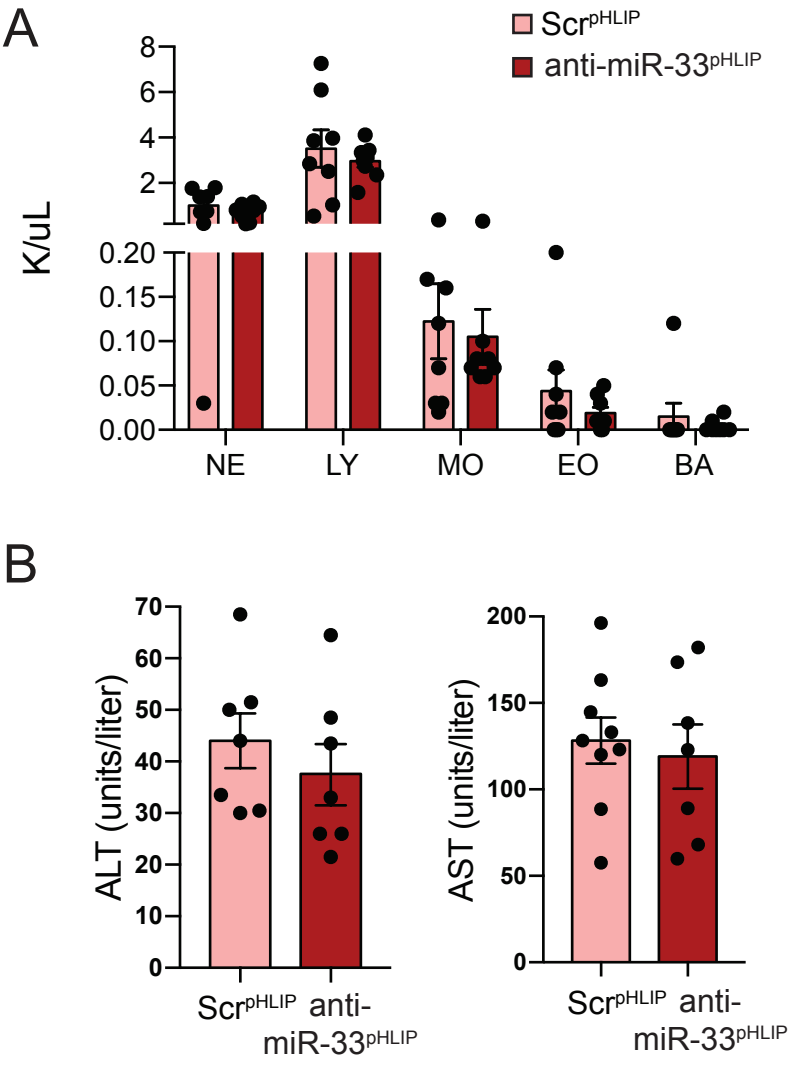
A
Scr pHLIP
anti-miR-33 pHLIP
K/uL
8
6
4
2
0.20
0.15
0.10
0.05
0.00
NE
LY
MO
EO
BA
B
ALT (units/liter)
70
60
50
40
30
20
10
0
Scr pHLIP
anti-miR-33 pHLIP
AST (units/liter)
200
150
100
50
0
Scr pHLIP
anti-miR-33 pHLIP

Figure S8

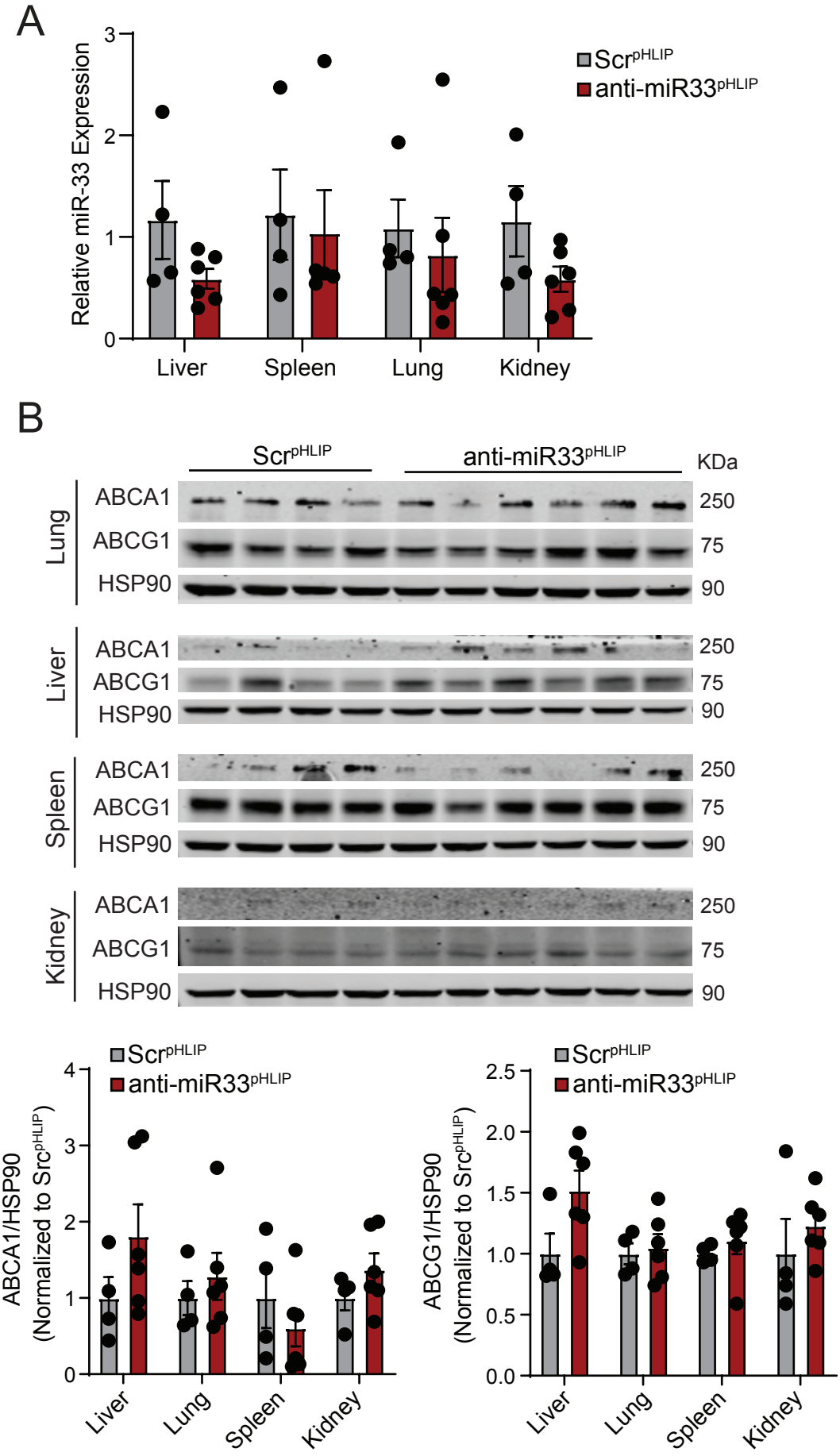
A
Relative miR-33 Expression
Scr pHLIP
anti-miR33 pHLIP
Liver
Spleen
Lung
Kidney
B
Scr pHLIP
anti-miR33 pHLIP
KDa
Lung
Liver
Spleen
Kidney
ABCA1
ABCG1
HSP90
250
75
90
ABCA1/HSP90 (Normalized to Src pHLIP)
ABCG1/HSP90 (Normalized to Src pHLIP)

Figure S9

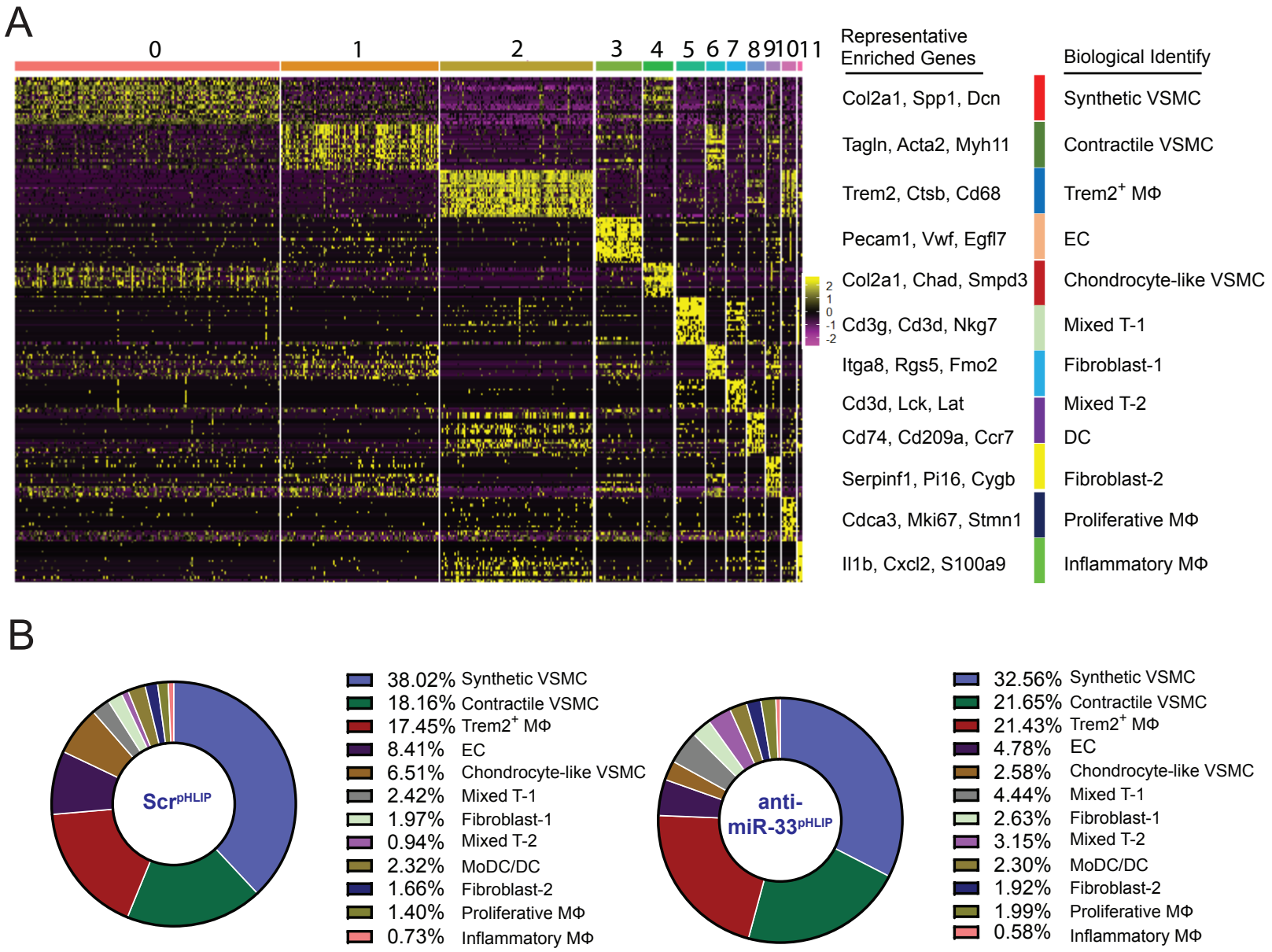
A
0
1
2
3
4
5
6
7
8
9
10
11
2
1
0
-1
-2
Representative Enriched Genes
Biological Identify
Col2a1, Spp1, Dcn
Synthetic VSMC
Tagln, Acta2, Myh11
Contractile VSMC
Trem2, Ctsb, Cd68
Trem2+ MΦ
Pecam1, Vwf, Egfl7
EC
Col2a1, Chad, Smpd3
Chondrocyte-like VSMC
Cd3g, Cd3d, Nkg7
Mixed T-1
Itga8, Rgs5, Fmo2
Fibroblast-1
Cd3d, Lck, Lat
Mixed T-2
Cd74, Cd209a, Ccr7
DC
Serpinf1, Pi16, Cygb
Fibroblast-2
Cdca3, Mki67, Stmn1
Proliferative MΦ
Il1b, Cxcl2, S100a9
Inflammatory MΦ
B
ScrpHLIP
38.02% Synthetic VSMC
18.16% Contractile VSMC
17.45% Trem2+ MΦ
8.41% EC
6.51% Chondrocyte-like VSMC
2.42% Mixed T-1
1.97% Fibroblast-1
0.94% Mixed T-2
2.32% MoDC/DC
1.66% Fibroblast-2
1.40% Proliferative MΦ
0.73% Inflammatory MΦ
anti-miR-33pHLIP
32.56% Synthetic VSMC
21.65% Contractile VSMC
21.43% Trem2+ MΦ
4.78% EC
2.58% Chondrocyte-like VSMC
4.44% Mixed T-1
2.63% Fibroblast-1
3.15% Mixed T-2
2.30% MoDC/DC
1.92% Fibroblast-2
1.99% Proliferative MΦ
0.58% Inflammatory MΦ

Figure S10

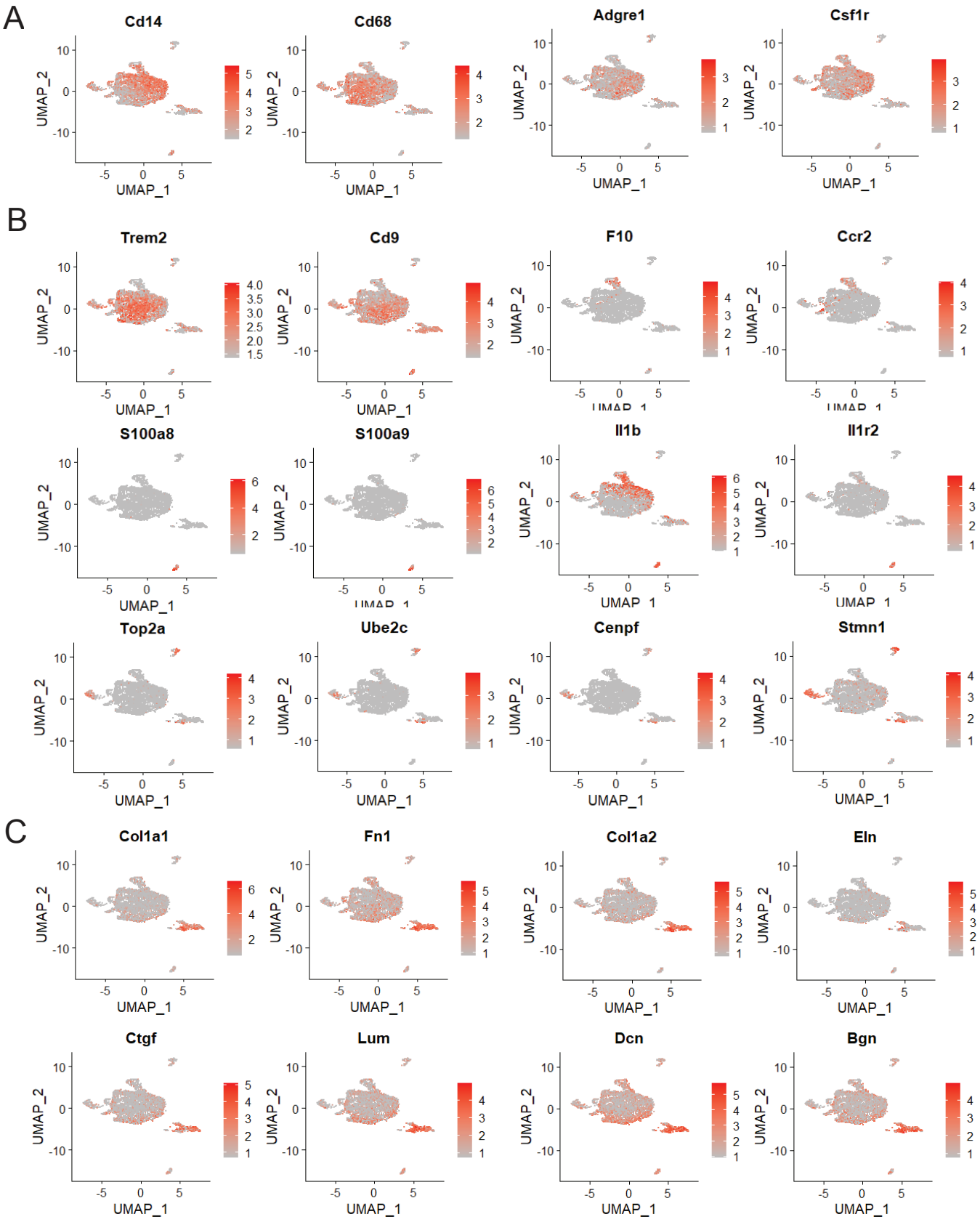
A
Cd14
Cd68
Adgre1
Csf1r
B
Trem2
Cd9
F10
Ccr2
S100a8
S100a9
Il1b
Il1r2
Top2a
Ube2c
Cenpf
Stmn1
C
Col1a1
Fn1
Col1a2
Eln
Ctgf
Lum
Dcn
Bgn
UMAP_1
UMAP_2